Dear Reviewers:

We greatly appreciate the reviewer's efforts in reviewing our manuscript. All the comments are very valuable for improving our manuscript. Below are the detailed point-by-point responses to the review comments. For clarity, the referees' comments are listed in black italics, and our responses and changes in the manuscript are shown in blue. We also mention where we made necessary changes in the revised manuscript by indicating page and line numbers in our responses. Please find our point-by-point responses below.

Response to Reviewer #3

This manuscript improved the parameterization scheme in terms of topography and cloud multi-scattering and generated a 1-km DSR product over the Tibetan Plateau. The topic is interesting and the DSR generation over Tibetan Plateau has been a great challenge over years. Overall, this study achieved high-accuracy DSR estimation over Tibetan Plateau, yet some details need to be clarified. I hope the authors could conduct some of my suggestions and comments, which may help to make this study much better.

Author Response: Thank you very much for your valuable suggestions and thoughtful instructions. All comments were helpful for improving our manuscript. We carefully revised the manuscript and made the following point-by-point revisions according to your suggestions.

Major concerns:

1. *In L134, as far as I know, MCD18A1 now offers a 1 km daily DSR. Letu et al. (2022) also generated a DSR product with topographic consideration at 10-min and 0.05° over East Asia-Pacific. I would like to know what is the advantage of the generated DSR in this study compared with them. A comparison with them would enhance the superiority of this study. See Letu et al. (2022) A New Benchmark for Surface Radiation Products over the East Asia–Pacific Region Retrieved from the Himawari-8/AHI Next-Generation Geostationary Satellite.*

Author Response: Thank you for this comment. The comparison results with MCD18A1 and Letu et al. (2020) have been added to Table 4. It should be noted that there are many missing values over the TP in MCD18A1. The same phenomenon was

found in Li et al. (2022). Fig. 1 will not be added to the revised manuscript, as it is only shown here to illustrate that there are many missing values over the TP in MCD18A1. To avoid the potential uncertainty caused by different sample sizes, the results given in Table 4 are of the same sample size.

The DSR product generated by Letu et al. (2022) (short for "H-8_EAP") is based on the Himawari-8/AHI satellite at a 10-min temporal scale and 5-km spatial scale over the East Asia-Pacific. The earliest time covered by this product was 2016. At present, the latest in situ data in this study are in 2016. In addition, the Himawari-8 satellite cannot observe the western part of the TP. The spatial range of the product cannot cover the entire TP. Therefore, six stations (BJ, QOMS, SETORS, NAMORS, NLGS and NLTS) in 2016 are selected to compare our product with H-8_EAP.

The RMSEs of MCD18A1 at three temporal scales are 233.47, 147.04 and 130.24 W m^{-2}, respectively. The MBs of MCD18A1 at three temporal scales are -76.43, -74.60 and -74.17 W m^{-2}, respectively. The estimates of this study show smaller RMSEs (152.13, 77.24 and 63.79 W m^{-2}) and lower absolute value MBs (5.23, 7.35 and 63.79 W m^{-2}). For H-8_EAP, the RMSEs at three temporal scales are 197.89, 140.67 and 125.70 W m^{-2}, respectively. The MBs at three temporal scales are -52.47, -57.07 and -62.74 W m^{-2}, respectively. The estimates of this study show smaller RMSEs (140.54, 82.67 and 71.48 W m^{-2}) and lower absolute value MBs (23.64, 21.54 and 14.97 W m^{-2}).

Table 4. Comparison with existing DSR products on different timescales in terms of accuracy.

Product name	Instantaneous timescale			Ten-day timescale			Monthly timescale			Spatial resolution
	RMSE (W m^{-2})	MB (W m^{-2})	R	RMSE (W m^{-2})	MB (W m^{-2})	R	RMSE (W m^{-2})	MB (W m^{-2})	R	
MCD18A1	233.47	-76.43	0.60	147.04	-74.60	0.72	130.24	-74.17	0.74	1 km
This study	152.13	5.23	0.72	77.24	7.35	0.82	63.79	7.25	0.84	
H-8_EAP	197.89	-52.47	0.66	140.67	-57.07	0.67	125.70	-62.74	0.73	5 km
This study	140.54	23.64	0.77	82.67	21.54	0.78	71.48	14.97	0.81	
ERA5	165.67	-20.59	0.65	88.06	-21.44	0.82	74.19	-21.06	0.86	25 km
This study	135.11	15.67	0.77	75.01	15.24	0.83	67.12	15.75	0.83	
CERES_SYN_1h	146.64	-46.70	0.75	84.27	-47.93	0.86	73.25	-47.53	0.89	100 km
CERES_SYN_3h	160.50	-78.30	0.74	107.13	-79.48	0.85	98.67	-79.06	0.88	
GEWEX_SRB	194.45	-118.56	0.68	143.68	-119.71	0.80	135.54	-119.21	0.83	
This study	132.84	2.79	0.77	70.84	2.18	0.84	61.33	2.70	0.85	

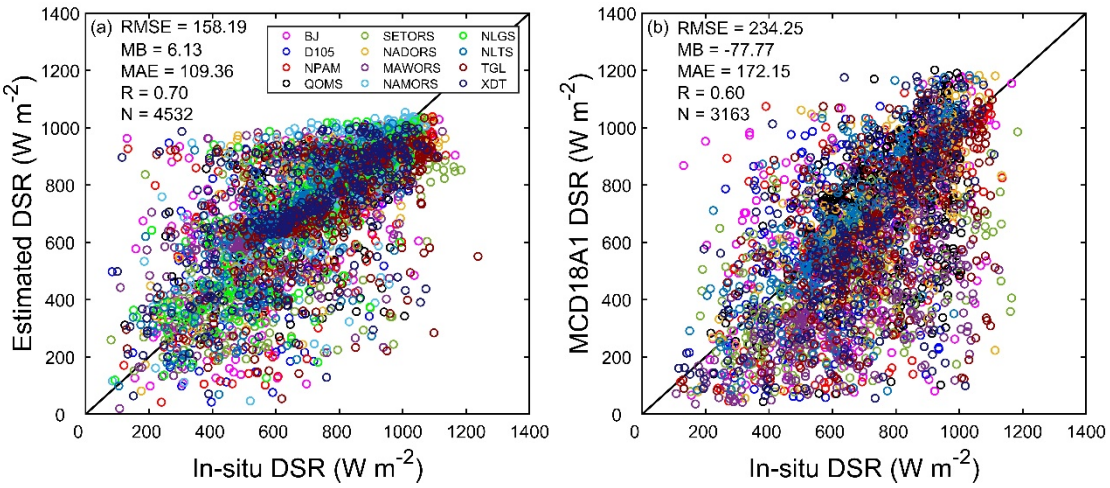

Figure 1. Comparison between the estimated instantaneous DSR and in situ measurements for (a) this study and (b) MCD18A1. N indicates the number of points. The legend with different colors denotes the twelve stations involved in the validation. The units of RMSE, MB and MAE are W m^{-2}.

Considering the available years of different DSR products, as well as the integrity and temporal continuity of in situ data, the MCD18A1 product was added to the comparison. The corresponding Figure 4 has been updated in the revised manuscript. Compared with other products, the DSR derived in this study is more consistent with the in situ observations at each station, and all show similar temporal change trends.

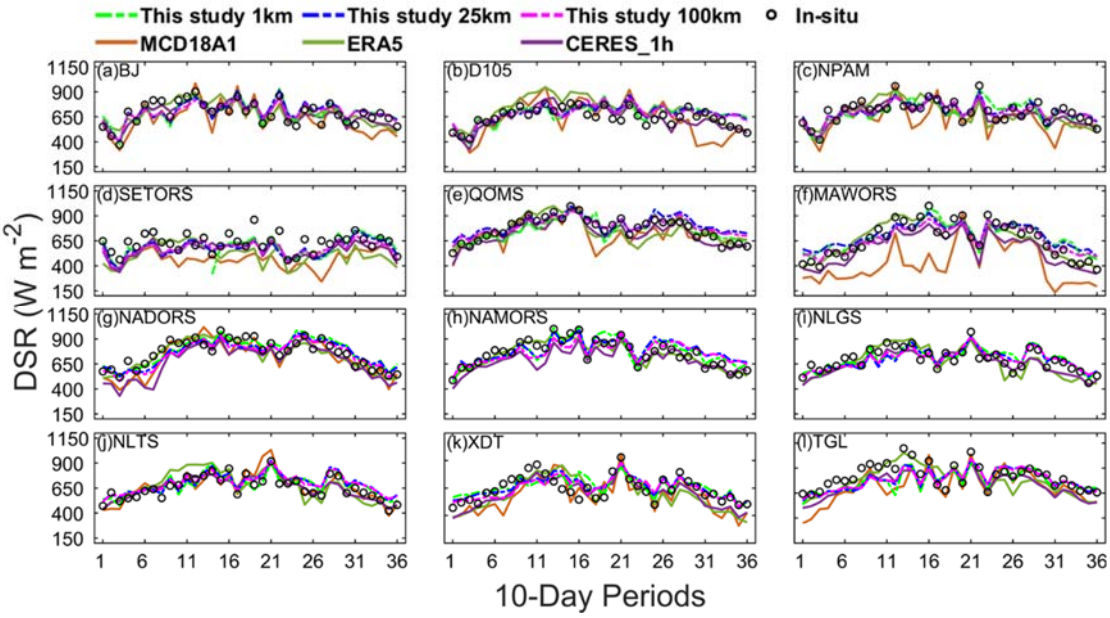

Figure 4. Intercomparison of time series of DSR among MCD18A1, ERA5, CERES_SYN_1 h, and this study at (a) BJ, (b) D105, (c) NPAM, (d) SETORS, (e) QOMS, (f) MAWORS, (g) NADORS, (h) NAMORS, (i) NLGS, (j) NLTS, (k) XDT, and (l) TGL stations on a ten-day timescale. The circle denotes in situ data.

Relevant statements have been updated in the revised manuscript as follows. (P14, L301-L312; P15, L323-L331; P16, L345-L348; P16, L353-354).

'Among these products, there are remotely sensed and reanalysis DSR products, namely, Clouds and the Earth's Radiant Energy System Synoptic (CERES_SYN) surface fluxes (Loeb et al., 2013), Global Energy and Water Exchanges Surface Radiation Budget (GEWEX_SRB) datasets (Zhang et al., 2014), MODIS DSR product (MCD18A1) (Wang et al., 2020) and the fifth generation reanalysis (ERA5) from the European Centre for Medium-Range Weather Forecasts (ECMWF) (Hans et al., 2019). In addition, Letu et al. (2022) produced a high-resolution (5 km, 10 min) DSR dataset (short for "H-8_EAP" in our study) under all-sky conditions from 2016 to 2020 in the East Asia–Pacific region based on the next-generation geostationary satellite Himawari-8/AHI, which was also selected for comparison. At present, the latest in situ data in this study are in 2016, and the Himawari-8 satellite cannot observe the western part of the TP. Therefore, six stations (BJ, QOMS, SETORS, NAMORS, NLGS and NLTS) in 2016 are selected for comparison with the H-8_EAP DSR dataset.' (P14, L301-L312)

'As summarized in Table 4, the RMSE range of these DSR products is approximately 150~230 W m^{-2} at the instantaneous scale. At the ten-day scale, the RMSE range is approximately 80~150 W m^{-2}. At the monthly scale, the RMSE range is approximately 70~130 W m^{-2}. The MB range of these DSR products is -120 ~ -20 W m^{-2} at three temporal scales. These large spans of RMSE and MB indicate that the current DSR products still have great uncertainties over the TP. The RMSE ranges of this study at three temporal scales are 132~152, 70~82 and 61~71 W m^{-2}. The MB range of this study is 3 ~ 24 W m^{-2} at three temporal scales. The estimates of this study show a smaller RMSE, lower absolute value MB and comparable R values at the corresponding spatial and temporal scales. This means that the derived DSR based on the proposed method performs better than other DSR products over the TP.' (P15, L323-L331)

'DSR products with relatively high accuracy, which correspond to three spatial resolutions of 1 km, 25 km and 100 km, are selected for comparison with the estimated DSR in this study in terms of temporal variation characteristics (Fig. 4). The time series of MCD18A1 at NAMORS and NLGS stations are not displayed because there are many missing values in MCD18A1 at these two stations.' (P16,

L345-L348)

'The dynamic range (defined as the difference between the maximum and the minimum in a year) of MCD18A1 is the largest, while ERA5, CERES_SYN_1 h and this study show similar dynamic ranges.' (P16, L353-354)

The related reference has been added in the revised manuscript as follows (P32, L718; P37, L855):

Letu, H., Nakajima, T. Y., Wang, T., Shang, H., Ma, R., Yang, K., Baran, A. J., Riedi, J., Ishimoto, H., Yoshida, M., Shi, C., Khatri, P., Du, Y., Chen, L., and Shi, J.: A new benchmark for surface radiation products over the East Asia–Pacific region retrieved from the Himawari-8/AHI next-generation geostationary satellite, Bulletin of the American Meteorological Society, 103, E873-E888, 10.1175/bams-d-20-0148.1, 2022. (P32, L718)

Wang, D., Liang, S., Zhang, Y., Gao, X., Brown, M. G. L., and Jia, A.: A new set of MODIS land products (MCD18): Downward shortwave radiation and photosynthetically active radiation, Remote Sensing, 12, 10.3390/rs12010168, 2020. (P37, L855)

2. *For Table 1, this method relied on atmospheric products, so a sensitivity analysis could be conducted to show the reliability and possible issues of the method. For example, introduce 10% random errors (this error depends on the performances of atmospheric products) to the input, and see how much the estimation result change.*

Author Response: Thank you for this comment. The accuracy of the parameterization scheme depends on the quality of the input data to some extent. To further understand the effect of uncertainties in input variables on the accuracy of the DSR retrieval scheme, sensitivity analysis of the DSR to input variables is conducted (Fig. 9 and Fig. 10). As shown in Fig. 8, three points located in the west, north central, and southeast of the TP are randomly selected for sensitivity tests. The average of each input variable (including air temperature Tair, air pressure Pair, specific humidity SH, ozone layer thickness, aerosol optical depth AOD, surface albedo, cloud effective radius CER and cloud water path CWP) for three randomly selected points is selected as the default value.

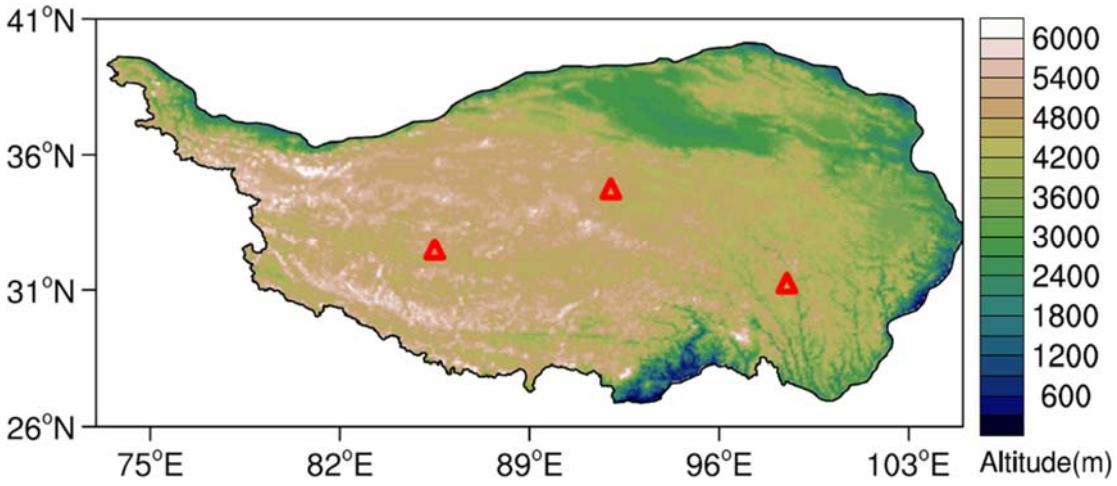

Figure 8. Locations of the three points (marked by red triangles) used to carry out sensitivity tests of the input data. The legend of the color map indicates the elevation above mean sea level in meters.

As shown in Fig. 9 and Fig. 10, in terms of changing trend and range, DSR has different responses to fluctuations of each input variable under different sky conditions. The sensitivity test results show that the DSR exhibits a positive correlation with Pair and ozone layer thickness and a negative correlation with Tair under both clear and cloudy conditions, with a nearly linear relationship (Fig. 9a, b, d and Fig. 10a, b, d). The DSR exhibits a negative correlation with SH and AOD with a nonlinear relationship under both clear and cloudy conditions (Fig. 9c,e and Fig. 10c,e). In addition, the DSR exhibits a positive correlation with CER and a nonlinear negative correlation with CWP under cloudy sky conditions (Fig. 10g and h). However, the DSR exhibits a linear positive correlation with surface albedo under clear sky conditions, while it displays a nonlinear positive correlation under cloudy sky conditions (Fig. 9f and Fig. 10f). This phenomenon indicates that multiple scattering effects occur between the atmospheric medium (aerosols and clouds) and the land surface (Ma et al., 2020).

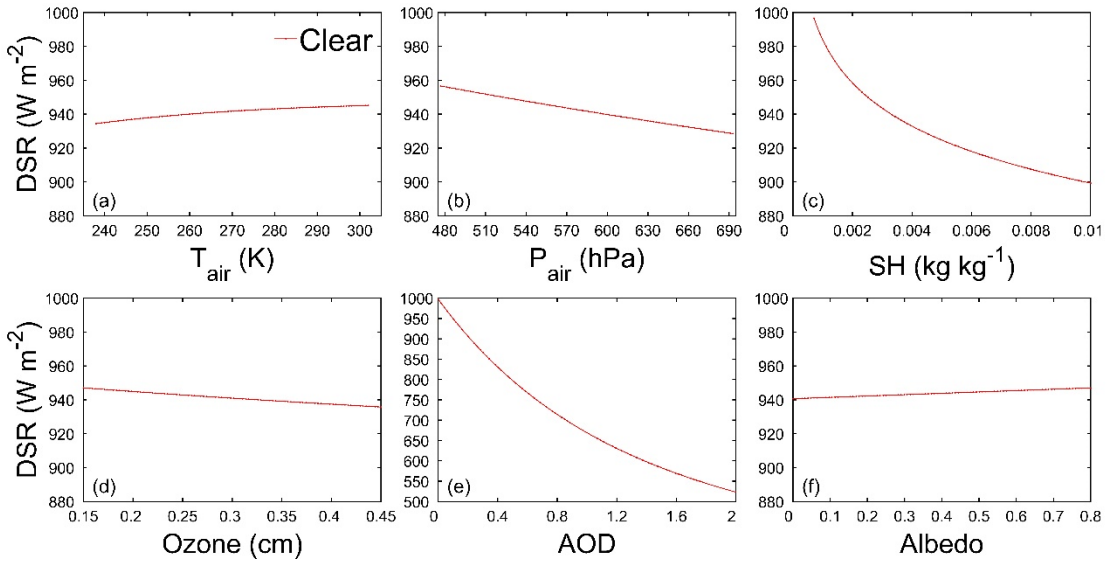

Figure 9. Sensitivity of DSR to (a) air temperature T_{air}, (b) air pressure P_{air}, (c) specific humidity SH, (d) ozone layer thickness, (e) aerosol optical depth AOD and (f) surface albedo under clear sky conditions.

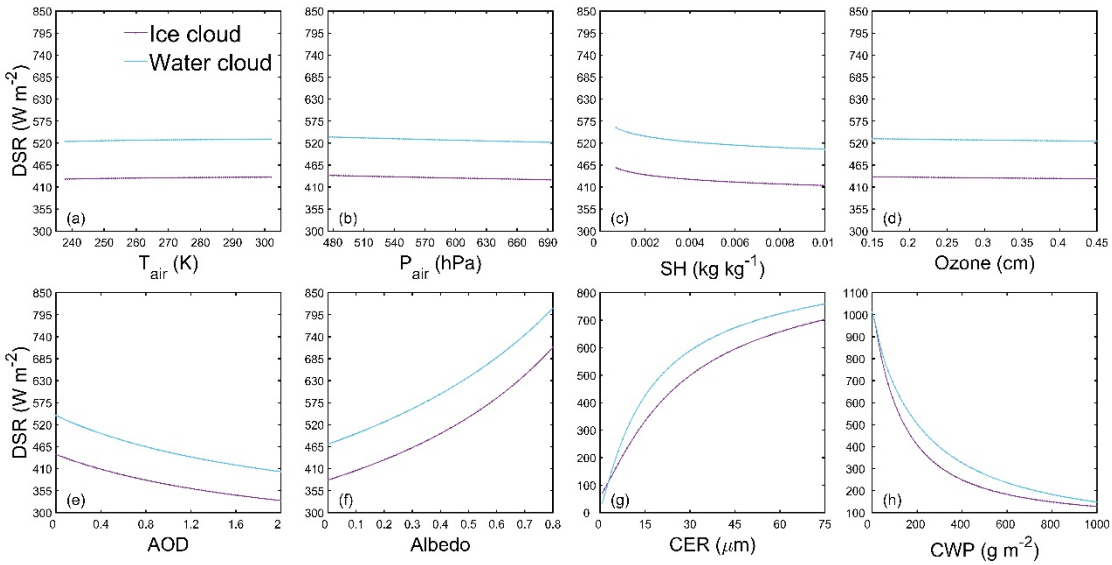

Figure 10. Sensitivity of DSR to (a) air temperature T_{air}, (b) air pressure P_{air}, (c) specific humidity SH, (d) ozone layer thickness, (e) aerosol optical depth AOD, (f) surface albedo, (g) cloud effective radius CER and (h) cloud water path CWP under cloudy sky conditions for ice clouds (purple line) and water clouds (blue line).

Moreover, the fluctuating range of input variables within one standard deviation (1σ) and the induced DSR fluctuation under different sky conditions are summarized in Table 6. Under clear sky conditions, the DSR is highly sensitive to AOD and SH and only slightly sensitive to other input variables. The AOD and SH within 1σ correspond to ranges of approximately 0-0.23 and 0.0004-0.0047 kg kg^{-1}, respectively, which would lead to DSR fluctuating by approximately 100.6 W m^{-2} and 87.4 W m^{-2}, respectively. Other input variables only induce fluctuations in DSR smaller than 15 W

m^{-2}. Under cloudy sky conditions, the DSR shows significant sensitivity to CWP and CER, moderate sensitivity to albedo, SH and AOD, and slight sensitivity to other input variables. The CWP within the 1σ range would lead to DSR fluctuating by approximately 768.1 W m^{-2} and 526.7 W m^{-2} for ice clouds and water clouds, respectively. The CER within the 1σ range would lead to DSR fluctuating by approximately 212.2 W m^{-2} and 202.3 W m^{-2} for ice clouds and water clouds, respectively. The magnitude of DSR fluctuations induced by the remaining input variables is much smaller than that caused by CWP and CER. In addition, the sensitivity of DSR to albedo is higher under cloudy sky conditions than under clear sky conditions, while the sensitivity of DSR to AOD and SH is lower under cloudy sky conditions than under clear sky conditions.

Table 6. Fluctuating range of input variables within one standard deviation (1σ) and the induced DSR fluctuation under clear sky and cloudy sky conditions.

	Clear		Ice cloud		Water cloud	
Variables	Ranges of variables within 1σ	DSR fluctuation range (W m^{-2})	Ranges of variables within 1σ	DSR fluctuation range (W m^{-2})	Ranges of variables within 1σ	DSR fluctuation range (W m^{-2})
T_{air} (K)	264-282	2.6	263-282	1.3	271-288	1.1
P_{air} (hPa)	530-622	-12.0	537-633	-4.9	550-646	-5.7
SH (kg kg^{-1})	0.0004-0.0047	-87.4	0.0006-0.0059	-38.0	0.0035-0.0083	-17.34
Ozone (cm)	0.25-0.28	-1.3	0.25-0.30	-0.7	0.25-0.28	-0.6
AOD	0-0.23	-100.6	0.03-0.21	-19.7	0.06-0.23	-21.1
Albedo	0.09-0.32	1.8	0.08-0.35	82.9	0.06-0.29	65.7
CER (μm)	-	-	16.7-39.8	212.2	9.3-21.4	202.3
CWP (g m^{-2})	-	-	0-409.6	-768.1	29.8-351.1	-526.7

In general, the inputs of cloud parameters CWP and CER are crucial variables, and their sensitivities are consistently high. AOD, surface albedo and SH are of secondary importance, with moderate sensitivity. AOD and surface albedo are more sensitive to DSR estimation than SH. Tair, Pair and ozone layer thickness only have a slight sensitivity to DSR estimation, in which ozone layer thickness is the least sensitive. The sensitivity test results indicate that the uncertainties in the input data of cloud parameters, aerosol parameters, surface albedo, and water vapour content are important error sources in the estimation of DSR (Huang et al., 2020; Letu et al., 2020).

The above information has been added to the revised manuscript (P22, L459-P24,

L513).

3. *In Table 2, could you please offer the slope and aspect of the stations? Here is a big concern that most stations are located in relatively flat areas in mountains, and as Figure 7 showed that DSR varied greatly with different terrain conditions, the 1 km* 1 km pixel has sub-topography, and the ground-measured shortwave flux could not represent the pixel-scale DSR in mountains. I think it is a great challenge to evaluate DSR products over mountainous areas. See Yan et al. (2020) An Operational Method for Validating the Downward Shortwave Radiation Over Rugged Terrains.*

Author Response: Thank you for this comment. The slope and aspect of the stations are listed in the Table 1.

Table 1. The slope (unit: degree, 0-90) and aspect (unit: degree, change between -180 and 180 from north to west, south and north in anticlockwise direction) information of the station.

Site	Slope(° from horizontal)	Aspect(° from north)
BJ	0.01	0.79
D105	0.03	-1.81
NPAM	0.01	2.55
QOMS	0.09	2.00
SETORS	0.18	0.93
MAWORS	0.01	-0.30
NADORS	0.01	-2.25
NAMORS	0.02	2.69
NLGS	0.00	2.55
NLTS	0.00	2.15
XDT	0.05	0.29
TGL	0.04	-2.24

According to the slope and aspect calculated based on DEM data, it can be considered that most stations are located on flat surfaces. It is true that evaluating DSR products over mountainous areas is a great challenge. Yan et al. (2020) proposed a methodology to validate DSR in mountainous areas. The premise of this method is that more than three stations are required on different slopes within kilometer-scale areas with rugged terrain (Yan et al. 2020). Currently, there are no such measurements on the TP, which makes it difficult to validate DSR, as the reviewer mentioned. For well-known reasons, setting up such measurements over the TP with extremely high altitude and harsh climatic environment is very costly and difficult.

4. *In Table 3, could you provide the sample size of each site at each timescale? I find that the sample size in Figure 3 was not large (N=155 on monthly scale), so I am afraid the different performances were attributed to the sample size in the validation.*

Author Response: Thank you for this comment. We have added the sample size of each site at each timescale to Table 3. At the same temporal scale, the sample size for each site does not differ significantly. Therefore, we believe that the sample size has little impact on the final validation result.

Table 3. Summary statistics of the validation results for each station on different timescales.

Site	Instantaneous timescale				Ten-day timescale				Monthly timescale				CCD
	RMSE ($W\ m^{-2}$)	MB ($W\ m^{-2}$)	R	N	RMSE ($W\ m^{-2}$)	MB ($W\ m^{-2}$)	R	N	RMSE ($W\ m^{-2}$)	MB ($W\ m^{-2}$)	R	N	
BJ	179.44	11.41	0.66	359	66.20	13.91	0.84	36	56.01	14.54	0.81	12	49.58%
D105	162.87	32.47	0.67	359	76.69	33.23	0.73	36	67.43	33.80	0.73	12	54.02%
NPAM	177.57	-3.90	0.63	358	67.63	-4.28	0.82	36	51.90	-3.75	0.82	12	53.46%
QOMS	112.33	5.04	0.74	689	56.49	6.38	0.90	69	49.76	6.41	0.91	23	19.83%
SETORS	183.33	-49.51	0.67	302	94.17	-49.48	0.67	33	64.89	-44.04	0.74	12	72.85%
MAWORS	167.41	28.51	0.71	350	83.27	27.08	0.90	36	72.94	27.32	0.92	12	55.62%
NADORS	129.88	19.48	0.78	318	66.20	17.59	0.89	36	58.30	18.20	0.90	12	35.07%
NAMORS	150.62	18.30	0.72	342	65.60	13.66	0.88	36	55.92	13.42	0.89	12	40.27%
NLGS	141.53	11.26	0.77	365	66.51	10.81	0.81	36	56.48	11.02	0.80	12	46.58%
NLTS	136.29	24.63	0.79	360	62.80	22.01	0.86	36	51.55	23.81	0.87	12	59.45%
XDT	183.08	17.84	0.63	365	81.41	17.95	0.72	36	70.48	18.02	0.70	12	51.23%
TGL	188.98	-46.64	0.58	365	97.70	-46.52	0.72	36	87.80	-46.92	0.66	12	45.63%

5. *In L525, did you consider the shelters from surrounding mountains to the target pixel's DSR? e.g., sky view factor and shadow. You can see that sky view factor matters, especially under cloudy sky: Ma et al. (2023) Estimation of fine spatial resolution all-sky surface net shortwave radiation over mountainous terrain from Landsat 8 and Sentinel-2 data.*

Author Response: Thank you for this comment. This parameterization scheme for calculating the DSR was improved by considering variations in the slope and azimuth of the land surface, as well as the terrain shadow in mountainous areas. The sky view factor was not taken into account in this study. Nevertheless, the radiation model over rugged terrains used in this study has already been validated in former studies. Therefore, we think it is feasible to use this model for the TP. Your suggestion of

introducing the sky view factor into the scheme may further improve the accuracy of the estimation. However, calculating solar radiation over rugged terrain is a complex task, as depicted in Ma et al. (2023), and more detailed considerations can be carried out in future work.

Here are some minor concerns:

1. *Could you be specific about what is high resolution (i.e., maybe < 5 km?) and what is coarse resolution in this study? Is the estimated DSR at an instantaneous scale? I am curious how you upscaled it to ten-day and monthly timescales for evaluation.*

Author Response: High resolution and coarse resolution are relative concepts that usually depend on the spatial coverage of the study area. For the TP, a spatial resolution finer than 5 km can be considered high resolution, and a spatial resolution coarser than 10 km can be considered coarse resolution. Since the main input data MODIS is at an instantaneous scale, the estimated DSR is also at an instantaneous scale. It is upscaled to ten-day and monthly timescales via arithmetic average for validation.

2. *In L62, I would like to know why the DSR could exceed the solar constant.*

Author Response: Due to its high altitude, low airmass and short path for solar radiation to reach the land surface, the TP receives a large amount of DSR. Coupled with multiple scattering of complex terrain, DSR can be higher than the solar constant. At the same time, if clouds that are conducive to scattering appear, the DSR could be higher than the solar constant due to reflection from clouds.

3. *In L116, the references in the 1990s are old, now many all-sky DSR products have been released.*

Author Response: The references have been updated in the revised manuscript. The references are as follows:

Huang, G., Li, Z., Li, X., Liang, S., Yang, K., Wang, D., and Zhang, Y.: Estimating surface solar irradiance from satellites: Past, present, and future perspectives, Remote Sensing of Environment, 233, 10.1016/j.rse.2019.111371, 2019.

Letu, H., Shi, J., Li, M., Wang, T., Shang, H., Lei, Y., Ji, D., Wen, J., Yang, K., and Chen, L.: A review of the estimation of downward surface shortwave radiation based on satellite data: Methods, progress and problems, Science China Earth

Sciences, 63, 774-789, 10.1007/s11430-019-9589-0, 2020.

4. *In L120, you mentioned many parameterization schemes did not consider the DSR attenuation caused by clouds carefully enough. This sentence is subjective, and could you please give some references? The next sentence should be improved, too.*

Author Response: Thank you for this comment. We have modified the sentence and added some references to the revised manuscript. (L120-L123)

'Second, some parameterization schemes did not consider the DSR attenuation caused by clouds carefully enough. Generally, only the single scattering of clouds was considered, and the multiple scattering effect of clouds was ignored (Huang et al., 2018; Huang et al., 2020).'

The references are as follows:

Huang, G., Liang, S., Lu, N., Ma, M., and Wang, D.: Toward a broadband parameterization scheme for estimating surface solar irradiance: Development and preliminary results on MODIS products, Journal of Geophysical Research: Atmospheres, 123, 12,180-112,193, 10.1029/2018jd028905, 2018.

Huang, G., Li, X., Lu, N., Wang, X., and He, T.: A general parameterization scheme for the estimation of incident photosynthetically active radiation under cloudy skies, IEEE Transactions on Geoscience and Remote Sensing, 58, 6255-6265, 10.1109/tgrs.2020.2976103, 2020.

5. *In L289, these DSR products need to be introduced in the Data Section. I think CERES_SYN_lh should be CERES SYNldeg-l Hour, am I right?*

Author Response: Yes, you are right. According to your suggestion, the introduction to the spatiotemporal resolution of different DSR products has been updated in the revised manuscript as follows (P14, L313-L314; P14, L316-L318).

'The spatial resolutions of MCD18A1 and ERA5 are 1 km and 25 km, respectively. CERES_SYN and GEWEX_SRB have a spatial resolution of 100 km.' (P14, L313-L314)

'The temporal resolution of MCD18A1 is instantaneous. GEWEX_SRB has a temporal resolution of 3 hours, and ERA5 has a temporal resolution of 1 hour. CERES_SYN products have two temporal resolutions of 1 hour and 3 hours.' (P14, L316-L318)